High-Power, Low-Internal-Reflection, Edge Emitting Light-Emitting Diodes

A new edge emitting LED has been developed for applications in optical low-coherence reflectometry. It offers improved sensitivity without introducing spurious responses.

by Dennis J. Derickson, Patricia A. Beck, Tim L. Bagwell, David M. Braun, Julie E. Fouquet, Forrest G. Kellert, Michael J. Ludowise, William H. Perez, Tirumala R. Ranganath, Gary R. Trott, and Susan R. Sloan

This article describes a new edge emitting LED (EELED) optimized for optical low-coherence reflectometry measurements.[1,2] Its use as a source for the HP 8504B precision reflectometer (see article, page 39) has resulted in improved measurement performance compared to the HP 8504A.

In optical low-coherence reflectometry, the output of a low-coherence source is coupled into an optical fiber and split in a 3-dB coupler as illustrated in Fig. 1. Half of the signal travels to a device under test (DUT), while the other half is launched into free space towards a mirror on a scanning translation stage. When the optical path length from the coupler to the mirror equals the optical path length from the coupler to a reflection in the DUT, the signals from the two arms add coherently to produce an interference pattern which is measured in the detector arm of the coupler. When the optical path length difference becomes larger than the coherence length of the source, this interference signal vanishes. The amplitude of the interference signal is proportional to the magnitude of the reflection from the DUT. Translating the mirror allows the reflectivity of the DUT to be mapped as a function of distance. With these new high-power EELEDs, the HP 8504B is able to measure return losses greater than 80 dB (reflections smaller than –80 dB) with a spatial resolution of 25 µm. In addition, reflections internal to the EELED have been reduced so that spurious signals are eliminated.

Source Characteristics

The important considerations in choosing a source for optical low-coherence reflectometry are spectral width, coherence length, spectral density, and output power. A broad spectral width implies a short coherence length and therefore a high spatial resolution capability. High output power and spectral density yield high sensitivity, that is, the ability to measure small reflections.

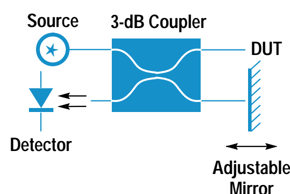

Fig. 1. Block diagram for optical low-coherence reflectometry measurements.

Many optical sources exhibit either a broad spectral width or high spectral density, but achieving both characteristics at the same time is more difficult. A tungsten-filament lamp has a very wide spectral width, but low spectral density (approximately –63 dBm/nm) when coupled into a single-mode fiber.[3] The amplified spontaneous emission (ASE) from an erbium-doped fiber amplifier (EDFA) provides a high spectral density (approximately 0 dBm/nm), but a narrower spectral width (30 nm).[4] EDFAs are relatively expensive and restricted to wavelengths near 1550 nm. Surface emitting LEDs provide moderate spectral density (approximately –45 dBm/nm) and broad spectral width (100 nm).[5]

EELEDs provide a relatively high spectral density (approximately –27 dBm/nm) with a spectral width of 40 nm to 80 nm. We chose the EELED for optical low-coherence reflectometry measurements because they offer a good balance of cost, power, and spectral width (spatial resolution).

An EELED is biased at a high drive current to achieve high output power. At elevated drive currents, undesirable internal reflections in commercially available EELEDs produce large spurious responses in optical low-coherence reflectometry measurements. Along with real reflections from the DUT, several undesired signals will be displayed, potentially confusing the interpretation of the reflection structure of the DUT.

We have succeeded in producing an EELED with reduced internal reflections, allowing high-sensitivity optical low-coherence reflectometry measurements to be made without spurious responses. The following sections describe the design and fabrication of this high-power, low-internal-reflection EELED.

Two-Segment EELED

Fig. 2 is a scanning electron micrograph (SEM) of the EELED structure. This InGaAsP/InP-based device uses a ridge structure. The ridge serves two functions in the device. It forms an optical waveguide, confining light in the direction parallel to the semiconductor surface. It also confines the pump current to be near the ridge. Fig. 3 shows a SEM and a pictorial diagram of the EELED cross section. The continuous ridge waveguide has two electrical contacts: a gain contact and an absorber contact. Under normal operation, the gain contact

© Hewlett-Packard Company 1995

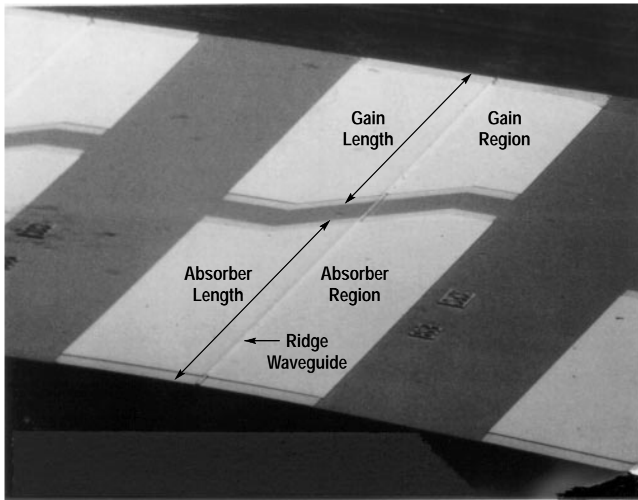

Fig. 2. Scanning electron micrograph (SEM) of the two-segment EELED.

is forward-biased and the absorber contact is reverse-biased. When a segment is forward-biased, an optical amplifier is formed. Under reverse bias, a highly absorbing optical detector is formed. The gain section generates amplified spontaneous emission (ASE) power at the device output facet from the forward traveling wave. The absorber section prevents the reverse traveling wave from reflecting off the back facet of the device. If the waves were allowed to reflect and circulate, the device could lase.

Organometallic vapor phase epitaxy (OMVPE) is used to grow the EELED epitaxial structure on InP (100) substrates. The first layer is an n-doped InP buffer. The light-emitting active region consists of an $In_{1-x}Ga_xAs_yP_{1-y}$ quaternary layer. The x and y fractions are chosen to provide the desired bandgap while maintaining lattice match to the InP substrate. Active region compositions for both 1300-nm and 1550-nm wavelengths have been developed. Zinc-doped p-InP is then grown above the active region. A heavily zinc-doped graded-bandgap layer is used to maintain low contact resistance to the top of the ridge.

The ridge location is first defined by a photolithographic process. The surrounding material is etched away in a CH_4/H_2 reactive ion etching chamber to a predetermined depth, stopping above the light-emitting active region. An electrically insulating silicon nitride layer is applied over the ridge structure. A window is opened in the silicon nitride on top of the ridge and a metal contact is deposited to form the topside gain and absorber electrodes. The semiconductor substrate is thinned to improve heat transfer and to facilitate cleaving. A backside metal is applied to form the substrate contact. The devices are finally cleaved to form the facets of the chip. More details on the processing steps are given in the article on page 20.

Operation and Spurious Responses

Fig. 4 shows the various paths that light can take to reach the EELED output facet. Two classes of signals can reach the device output. One is desired while the other is undesired. The undesired paths cause spurious responses during optical low-coherence reflectometry measurements.

Desired Path. When the gain region is forward-biased, light is spontaneously emitted isotropically from all points under the gain section. A fraction of the spontaneously emitted light is captured in the ridge waveguide. The spontaneous emission is amplified in both forward and reverse traveling waves. The desired output from the EELED is the forward traveling light (toward the output facet) with a single pass through the gain section. Most of the amplified spontaneous emission (ASE) leaving the output facet originates from the rear of the gain section (nearest the absorber) since these spontaneously emitted photons receive the largest amplification. An equal amount of ASE originates primarily at the forward end of the gain section and travels toward the absorber contact. An ideal absorber region prevents all of the reverse traveling ASE from reflecting off the back facet and becoming forward traveling energy. At the high pump currents used to drive the EELED, the absence of an absorber region could allow the device to lase. The source would then no longer have a broad, incoherent spectral width.

Undesired Paths. An undesired output occurs when photons reach the output along more than one path. These undesired paths start with a reflection from the output facet of the device. Although the output facet is antireflection-coated, such coatings are not perfect and some signal will be reflected. The signals reflected at the output facet travel back through the gain region toward the absorber section. An undesired output occurs if this signal is reflected a second time and travels back toward the device output. These twice-reflected signals will add to the desired output of the EELED and cause a spurious response. Possible sources of secondary reflections are distributed reflections along the length of the ridge waveguide, discrete reflections at the gain-to-absorber

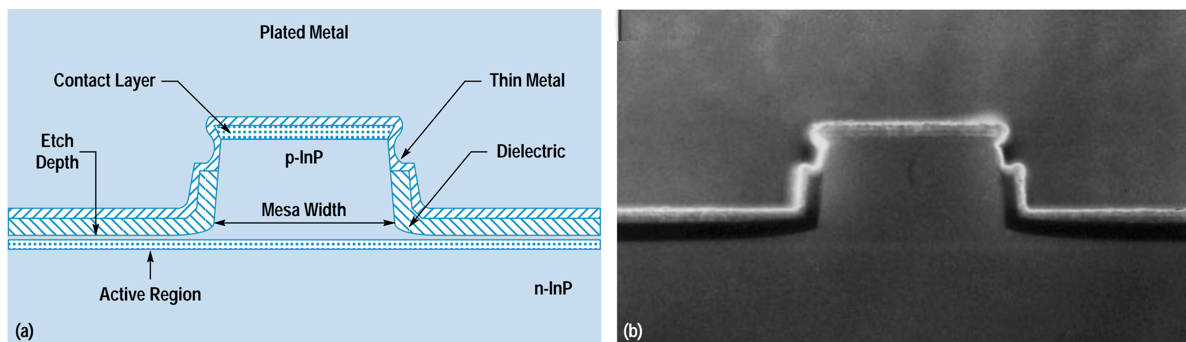

Fig. 3. (a) Cross section and (b) pictorial view of the ridge waveguide.

© Hewlett-Packard Company 1995

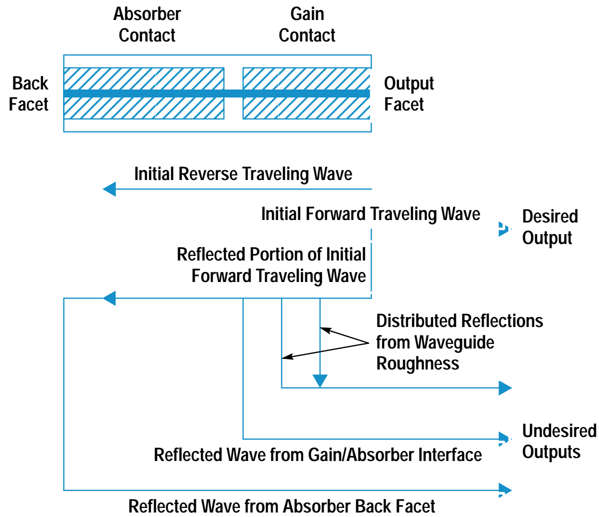

Fig. 4. Optical signal flow chart for the EELED.

interface, and discrete reflections at the back facet of the EELED.

If a source that has a large number of internal reflections is used to make an optical low-coherence reflectometry measurement, the resulting information can be confusing. Fig. 5 shows an optical low-coherence reflectometry measurement of a fiber-to-air reflection using an EELED source that has a significant level of internal reflections. This device is biased to deliver an output power of 40 μW. Ideally, the display would show only a single 15-dB return loss spike at the glass-to-air interface. The actual display shows several other spurious signals that arise from internal reflections in the device. The cause of each spurious response is identified in Fig. 5. The spurious responses appear symmetrically located about the true fiber tip reflection. The spacing between the spurious response and the fiber tip reflection is equal to the optical distance between the two reflection points in the undesired paths. Twice-reflected signals make up to three passes through the gain region, compared to one pass for the desired signal. Because of the three gain passes, the undesired signals rise very quickly as the gain and consequently

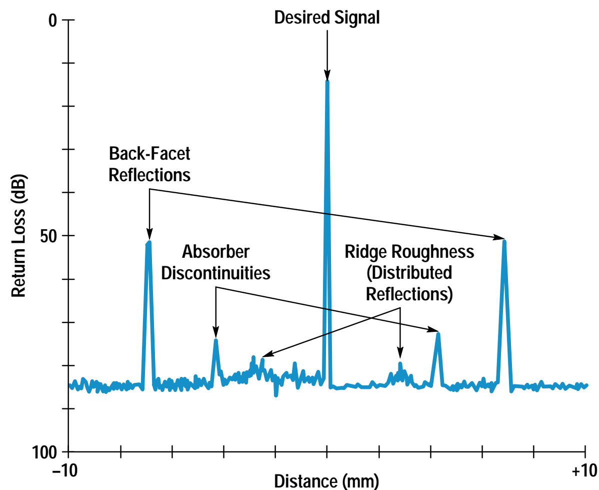

Fig. 5. Example of spurious signal generation in optical low-coherence reflectometry using a 1300-nm EELED source with a high level of internal reflections.

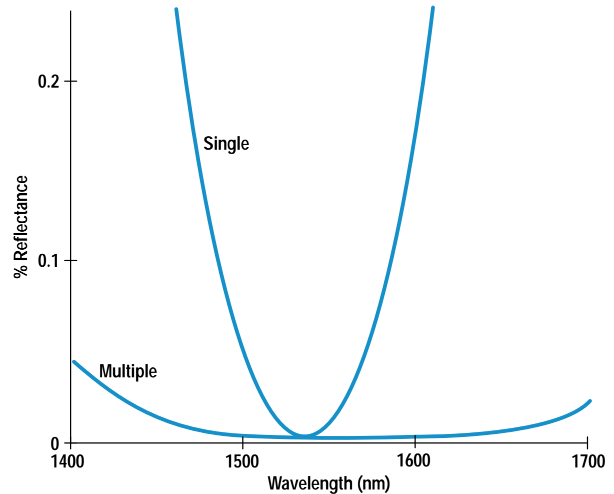

Fig. 6. Antireflection coating reflectivity versus wavelength for single-layer and multiple-layer designs.

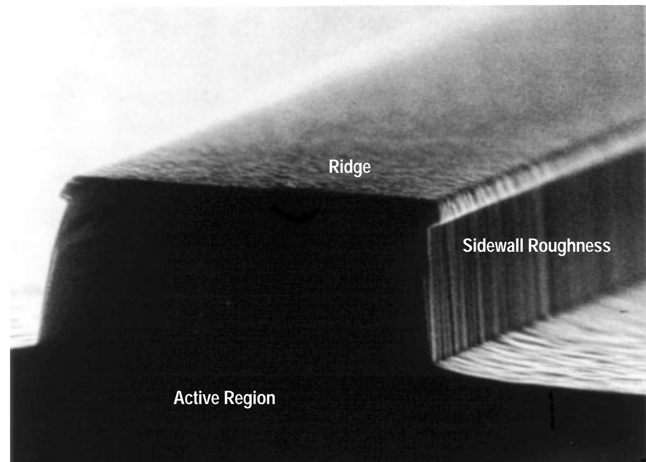

Fig. 7. SEM showing sidewall roughness in the ridge waveguide.

the power from the device are increased. For every 1 dB of increased output power, the spurious signals increase their level by 3 dB. Therefore, when attempting to use a high output power it is critically important to reduce all sources of internal reflection in the EELED. In the next section we will identify methods to minimize these internal reflections.

Reducing Reflections

It is very important to reduce the reflectivity of the output facet since all of the undesired twice-reflected signals depend directly on it. The wide spectral output of this device necessitates a broadband antireflection coating. Output facet antireflection coating reflectivity curves are shown in Fig. 6. The coating is made up of multiple layers, resulting in a broader low-reflectance window than a traditional single-layer, quarter-wavelength design.

The distributed reflections along the length of the optical waveguide are caused by variations in the ridge dimensions along the waveguide length. The conditions for the reactive ion etching of the ridge were chosen to minimize these waveguide variations. Fig. 7 shows the sidewalls and sloping floor of the ridge taken after the reactive ion etching process

© Hewlett-Packard Company 1995

step. There are small vertical striations in the sidewalls, but over a larger scale the surface is very smooth. The magnitude of the distributed reflections from these ridge striations is estimated to be at a level of less than 110 dB return loss. The distributed reflection level provides a lower limit to the multiple reflection characteristics of an EELED since a small amount of waveguide reflectivity is unavoidable.

Another source of secondary reflections exists at the gain/absorber interface. Since the gain section is heavily pumped and the absorber section is reverse-biased, the carrier density changes suddenly between these two sections. The index of refraction depends on the carrier density in semiconductors.[6] This abrupt change in carrier density can cause a reflection. An unbiased region between the gain and the absorber not only avoids conduction between the two sections, but also allows the carrier density (and thus the index of refraction) to taper off gradually, reducing the reflectivity. The gain contact is angled with respect to the waveguide to reduce the carrier density gradient and to direct any remaining reflection out of the waveguide.

The absorber characteristics are very important in obtaining low-internal-reflection EELEDs. The efficiency of the absorber at the long-wavelength end of the output spectrum is small. It is possible for deleterious levels of long-wavelength light to reflect off the back facet, thereby degrading optical low-coherence reflectometry performance. The characteristics of the absorber section have been measured experimentally and are presented in Fig. 8. The top curve shows the spectral density of the light from the EELED output facet as measured by an optical spectrum analyzer. The amount of light generated at long wavelengths is enhanced because of bandgap shrinkage and heating effects in the gain segment.[7] The output from the absorber section under several bias conditions is shown in the lower curves. The difference between the output curves and the absorber curves represents the absorption of the absorber segment as a function of wavelength. The absorber section effectively attenuates the light in the short-wavelength end of the output spectrum. The longer-wavelength light from the EELED travels through the absorber segment with relatively little absorption. Transmission through the absorber at long wavelengths is reduced by increasing the magnitude of the reverse bias on the absorber section. This increase in long-wavelength absorption is caused by the Franz-Keldysh effect[8] in bulk active region devices. We have also studied the absorber sections of devices using quantum well active regions. These devices use the quantum-confined Stark effect[9] to increase long-wavelength absorption. In our present bulk active region design, we have chosen a very long absorbing section. This reduces the back facet effective reflectivity to a level lower than that of the distributed reflection along the length of the gain section.

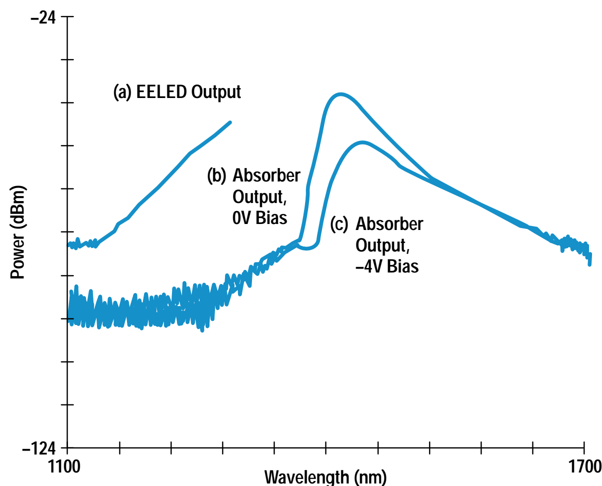

Fig. 8. (a) Gain segment output (forward traveling wave) as viewed in a 5-nm resolution bandwidth on an optical spectrum analyzer. (b) Output from the absorber section (reverse traveling wave) for a 0-volt bias and (c) a –4-volt bias.

Fig. 9 illustrates an optical low-coherence reflectometry measurement using the optimized EELED biased to produce an output power of about 40 μW, the same output power as the earlier device shown in Fig. 5. Fig. 9 shows a much lower level of internal reflections. The new EELED offers good sensitivity without the spurious responses that can be confused with real responses. If the output of the new EELED is increased to higher power (hundreds of microwatts), the spurious signals will eventually rise out of the noise floor, since spurious signals rise more quickly than the desired signals.

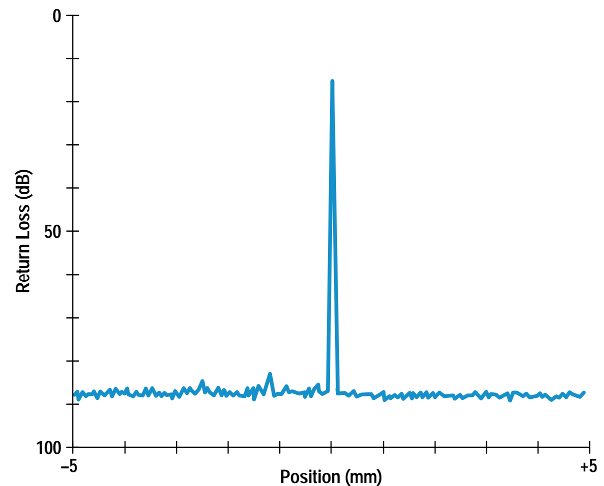

Fig. 9. Example of an optical low-coherence reflectometry measurement for an optimized 1300-nm EELED as described in this article.

Power Characteristics

The EELED must produce high output power while maintaining low internal reflections. Power translates directly into increased measurement sensitivity for optical low-coherence reflectometry applications. In designing a device for high-power applications the following parameters must be considered: gain section length, ridge waveguide dimensions, active region designs, and device mounting techniques.

The output power of an EELED depends on the gain achievable in the optical amplifier (gain section). High net gain can be achieved with either a large amount of gain per unit length from a shorter segment or a smaller amount of gain per unit length from a longer segment. Fig. 10 compares the pulsed output power from EELEDs with 300-μm and 800-μm gain segment lengths. The absorber section lengths for both devices were identical. In each case, the light-versus-current

© Hewlett-Packard Company 1995

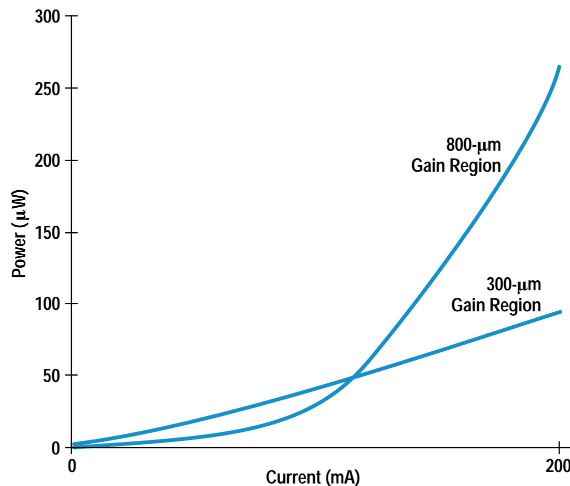

Fig. 10. Pulsed output power into a single-mode fiber versus current for 1550-nm EELEDs with gain section lengths of 300 μm and 800 μm.

curve is initially superlinear, meaning that the slope of the curve increases with drive current. At low current levels, the waveguide under the gain contact experiences a net loss per unit length, so that only the spontaneously emitted light near the output facet actually leaves the device. As drive current in the gain contact is increased, the device gain increases and the output power increases. The power output will eventually be limited by optical saturation of the gain region's output (by its own ASE), by nonradiative carrier recombination effects, by heating, or by a combination of these effects.

For lower drive currents, the device with the short gain region produces higher output power. For higher drive currents, the device with the longer gain region produces significantly higher output power. Under direct current bias conditions the output power difference between the short and long gain section lengths is even more dramatic. Several factors play a role in the increased output power from the longer device. The 300-μm device must obtain a large amount of gain in a short distance, requiring a higher current density and therefore a greater temperature rise than the longer device to achieve the same gain. The carrier density is also much higher for the shorter gain region length. As carrier density and temperature increase, a larger fraction of the pumping current goes into wasted nonradiative recombination compared to the desired radiative recombination. Auger recombination mechanisms are especially important at high carrier densities in the InGaAsP/InP material system and are more prominent in 1.55-μm devices than in 1.3-μm devices.[10]

The ridge design can also have a major effect on output power. We have investigated a variety of ridge widths ranging from a few to many micrometers. The narrower devices couple light more efficiently into single-mode fiber but the wider devices produce slightly lower levels of distributed reflections along the length of the gain section because the edge roughness lies farther away from the center of the waveguide. The ridge depth (distance from the ridge top to the material left above the active layer in the field as shown in Fig. 3) is also a key parameter in achieving a high output power. The depth controls both the transverse waveguiding of the optical mode and the current confinement in the device. Fig. 11 illustrates two extremes of etching. If the etch is not sufficiently deep, the current will spread so that a significant fraction of the current will be wasted pumping parasitic regions of the device in which the optical field is small. The optical mode will not be optimally confined. If the etch is too deep, the optical mode will intersect the lossy metal contacts, causing the waveguide loss to increase and output power to decrease. Etching into the active region can also introduce recombination losses. An optimal compromise between these two extremes was reached experimentally.

The output power capability of EELEDs with both quantum well and bulk active region structures has been studied.[2] For the same gain section lengths, bulk active region designs have produced higher power.

The spectral characteristics of the EELED depend on the amount of spontaneously emitted light captured in the waveguide at each wavelength and the bandwidth of the optical amplifier. Fig. 12 shows the spectral characteristics of a 1300-nm EELED and a 1550-nm EELED. The 1550-nm device exhibits a full width at half maximum (FWHM) spectral width of 56 nm at an output power of 350 μW. The 1310-nm device exhibits a FWHM of 51 nm at an output power of 80 μW.

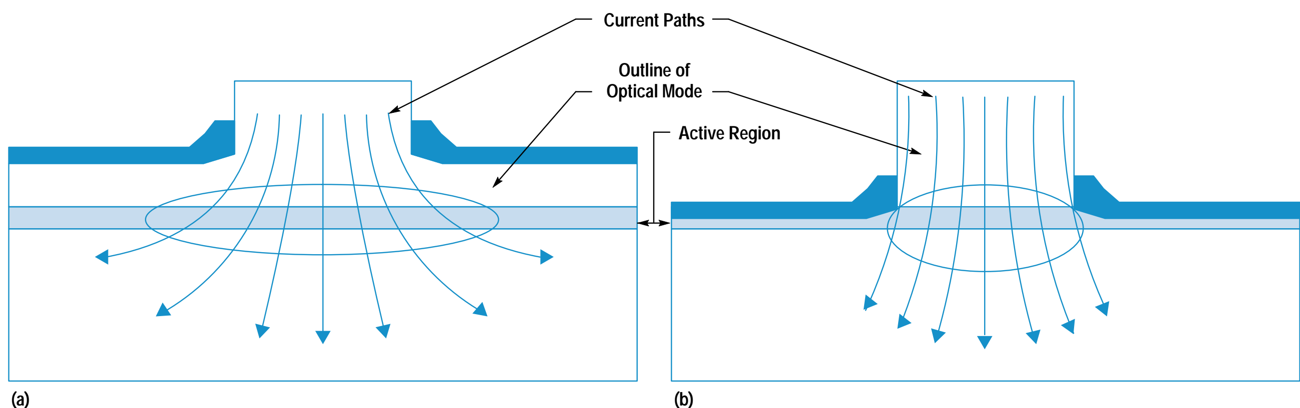

Fig. 11. Current and optical confinement for (a) shallow and (b) deep ridge etch.

© Hewlett-Packard Company 1995

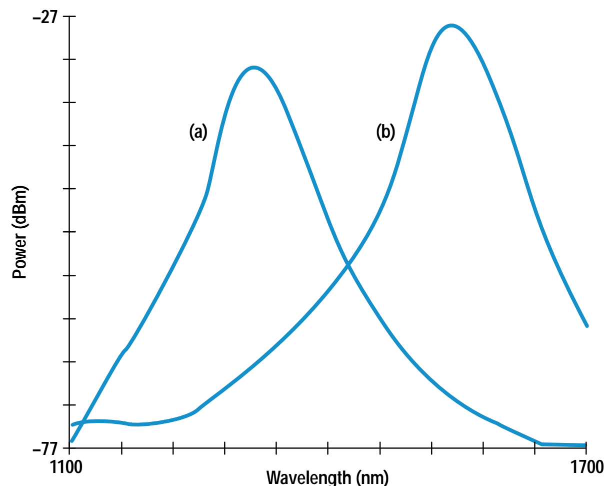

Fig. 12. Spectral characteristics of 800-μm-long gain section EELEDs at a current of 200 mA for (a) 1310-nm and (b) 1550-nm center wavelengths. The resolution bandwidth is 1 nm.

Reliability Results

Reliability of these ridge devices has been investigated, with over 6000 hours of accelerated life testing to date. Device failure is usually defined as a decrease of output power to one half of its initial value. Using this criterion, an extrapolation from measured data allows a lifetime prediction for the device. By measuring the lifetime at several temperatures we can determine the activation energy of the failure mode and infer what the actual lifetime will be at the operating temperature of the device. The lifetime of these devices is estimated to be over 800,000 hours at 25°C.

Summary and Conclusions

EELEDs optimized for optical low-coherence reflectometry applications have been developed. They are used in the HP 8504B precision reflectometer for increased measurement sensitivity and elimination of spurious signal responses in the display.

The devices have been optimized by reducing internal reflections and increasing output power. To reduce reflections we have: (1) produced smooth sidewalls on the optical waveguide during the ridge formation process, (2) extended the gain-to-absorber transition region and angled the metal contacts, (3) fabricated a long absorber section with the capability of applying a reverse bias to reduce back-facet reflections, and (4) applied a broadband antireflection coating to the output facet. The devices were also designed for increased power. The power was increased by: (1) employing a long gain section length, (2) optimizing the ridge etch depth, (3) choosing the ridge width as a compromise between efficient coupling to single-mode fiber and low distributed internal reflections, and (4) choosing a bulk active region design.

The characteristics that make these EELEDs valuable for optical low-coherence reflectometry also make them ideal sources for other applications requiring high power and low internal reflections. They could be used in fiber-optic gyroscopes, which require a very low-coherence source. In conjunction with an optical spectrum analyzer (such as the HP 71450/71451A), they can be used to measure the characteristics of optical components as a function of wavelength. Although 1300-nm and 1550-nm sources have been discussed because of their current importance to the telecommunications industry, EELEDs for other wavelengths between 1200 nm and 1700 nm can be produced by changing the epitaxy in the active region.

Acknowledgments

The authors would like to recognize the contributions of Nance Andring, Joan Henderson, Marilyn Planting, Mike Young, Henrietta Gamino, Johnny Ratcliff, and Shonna Close for processing the devices. Thanks go to Howard Booster, Bob Bray, George Patterson, Kent Carey, and Waguih Ishak for their strong support of this project.

References

1. H. Chou and W. Sorin, “High-Resolution and High-Sensitivity Optical Reflection Measurements Using White-Light Interferometry,” *Hewlett-Packard Journal,* Vol. 44, no. 1, February 1993, pp. 52-58.
2. J.E. Fouquet, G.R. Trott, W.V. Sorin, M.J. Ludowise, and D.M. Braun, “High-Power Semiconductor Edge Emitting Light-Emitting Diodes for Optical Low-Coherence Reflectometry,” *to be published in the IEEE Journal of Quantum Electronics.*
3. L.F. Stokes, “Coupling Light from Incoherent Sources to Optical Waveguides,” *IEEE Circuits and Devices Magazine,* January 1994, pp. 46-47.
4. W.V. Sorin and D.M. Baney, “Measurement of Rayleigh Backscatter at 1.55 μm with 32 μm Spatial Resolution,” *IEEE Photonics Technology Letters,* Vol. 4, no. 4, April 1992, pp. 374-376.
5. S.E. Miller and I.P. Kaminow, *Optical Fiber Communications II,* Academic Press, 1988, p. 467 ff.
6. J.I. Pankove, *Optical Processes in Semiconductors,* Dover, 1971, p. 89 ff and p. 392 ff.
7. G.P. Agrawal and N.K. Dutta, *Long-Wavelength Semiconductor Lasers,* Van Nostrand Reinhold Co., 1986, p. 28 and p. 86.
8. S. Wang, *Fundamentals of Semiconductor Theory and Device Physics,* Prentice Hall, 1989, p. 618 ff.
9. J.E. Fouquet, W.V. Sorin, G.R. Trott, M.J. Ludowise, and D.M. Braun, “Extremely Low Back Facet Feedback by Quantum Confined Stark Effect Absorption in an Edge Emitting Light-Emitting Diode,” *IEEE Photonics Technology Letters,* Vol. 5. no. 5, May 1993.
10. G.P. Agrawal and N.K. Dutta, *op cit,* p. 23 ff.

© Hewlett-Packard Company 1995